Investigations of the spin hamiltonian parameters and local structure for Cr^{3+} in K_2PdCl_4 single crystal

Xu-Sheng Liu[a], Shao-Yi Wu[a], Li-Na Wu[a], Li Peng[a], Li-Juan Zhang[a], and Hui-Ning Dong[b,*]
[a]*Department of Applied Physics, School of Physical Electronics, University of Electronic Science and Technology of China, Chengdu 610054, PR China*
[b]*College of Physics and Engineering, Chengdu Normal University, Chengdu 611130, P.R. China.*
[*]*e-mail: donghn69@163.com.*

Received 30 March 2017; accepted 25 July 2017

The spin Hamiltonian parameters (SHPs) (g factors and zero-field splittings (ZFSs) D and E) and the local structure for Cr^{3+} in K_2PdCl_4 single crystal are theoretically investigated from the perturbation calculations of the SHPs for an orthorhombically distorted octahedral $3d^3$ cluster. The impurity Cr^{3+} is found not to occupy the conventional square planar Pd^{2+} site but to locate at the octahedral K^+ site, associated with the relative axial compression ratio $\rho(\approx 11.1\%)$ and the perpendicular bond length variation ratio $\tau(\approx 11.7\%)$. The impurity centre exhibits much smaller axial compression distortion and much larger perpendicular orthorhombic distortion than the host K^+ site in K_2PdCl_4 ($\rho_H \approx 18.6\%$ and $\tau_H \approx 0$) and hence a more regular ligand octahedron, corresponding to the very small ZFSs. The contributions to g-shifts Δg_{CT} from the CT mechanism are opposite in sign and twenty-one times larger in magnitude compared with Δg_{CF} from the CF mechanism. For the ZFSs, the CT contributions D_{CT} and E_{CT} are opposite in sign and almost the same in magnitude with respect to the corresponding D_{CF} and E_{CF}.

Keywords: Electron paramagnetic resonance; defect structures; Cr^{3+}; K_2PdCl_4.

PACS: 61.72.Hh

1. Introduction

Palladium(II) complex K_2PdCl_4 has attracted considerable attention due to the medicinal properties as well as applications in drugs with high antitumoral and antibacterial activity [1]. Meanwhile, K_2PdCl_4 can act as a catalyst to afford an efficient, mild and environmentally friendly method in the synthesis of α-aminonitriles [2]. This material is also used in an increasing number of applications in chemical, electrical, electronic and glass industries and the manufacture of jewellery [3]. On the other hand,Cr^{3+} is a widely used dopant in various functional systems such as night-vision materials [4], fiberoptic thermometers [5], laser hosts [6,7], photocatalysis [8] as well as vivo imaging and drug delivery mediums [9]. Cr^{3+} is also essential for mammal metabolism with declining concentrations of both glycose and cholesterol in blood [10], and its non-specific binding with DNA and other cellular components can possibly result in inhibition of transcription and replication of DNA [11]. In addition, Cr^{3+} as an environmental contaminant and various industrial and agricultural activities (especially in food and water) has been a focus in the relevant fields [12,13].

Usually, the above properties and applications may strongly depend upon the electronic structures and local behaviors of Cr^{3+} in these systems, and the investigations on the local structures and behaviors of Cr^{3+} in K_2PdCl_4 are of scientific and practical significance. It is known that EPR spectroscopy is sensitive to the immediate environment around the paramagnetic impurities and able to reveal important microscopic information (*e.g.*, defect structures such as occupation, strength of crystal-fields and local lattice distortions etc.) in the hosts. Recently, electron paramagnetic resonance (EPR) study was carried out for Cr^{3+} doped K_2PdCl_4 at liquid nitrogen temperature (LNT), and the spin Hamiltonian parameters (SHPs) were measured for the orthorhombic substitutional Cr^{3+} centre on K^+ site (site I) [14]. So far, the above EPR experimental results for Cr^{3+-} doped K_2PdCl_4 have not been theoretically explained, except that the d-d transition optical spectra were quantitatively analyzed based on the crystal-field theory [14]. Since this orthorhombic Cr^{3+} centre on the host K^+ site in K_2PdCl_4 is quite different from the conventional tetragonal Cu^{2+} centre on square planar Pd^{2+} site, further theoretical investigations on the SHPs of this system can be helpful to understand the impurity behaviors and the properties of K_2PdCl_4 with transition-metal dopants and are of specific importance. The aim of this article is to propose satisfactory and uniform interpretations of the SHPs for the Cr^{3+} centre in K_2PdCl_4 by involving the local structure of the impurity based on the perturbation calculations of these parameters. The arrangement of this paper is the follows. In Sec. 2, the relevant theoretical formulas for the calculations of the SHPs are provided. The results are discussed in Sec. 3. The conclusion of the article is drawn in the last section.

2. Theoretical calculations

In this section, the theoretical calculations of the SHPs are performed for the Cr^{3+} centre in K_2PdCl_4. In the treatments, the contributions to the SHPs from both the crystal-field (CF)

and charge-transfer (CT) mechanisms are included in view of significant covalency of the system. EPR measurements [14] indicate that Cr^{3+} in K_2PdCl_4 occupies substitutionally the host K^+ site and exhibits the local orthorhombic (D_{2h}) site symmetry. For a $3d^3$ (Cr^{3+}) ion under orthorhombically distorted octahedra, its ground orbital singlet $^4A_{2g}$ may yield ZFSs D and E via the combination of the spin-orbit coupling and the orthorhombic CF interactions [15].

2.1. Cluster approach treatments involving both the CF and CT contributions

In view of the high valence state of central ion Cr^{3+} and the strong covalency of ligand Cl^-, the studied $[CrCl_6]^{3-}$ cluster may demonstrate strong covalency and CT contributions to the SHPs [15-17]. Based on the cluster approach [18,19] involving both the CF and CT contributions, the spin-orbit coupling coefficients and the orbital reduction factors are expressed as follows:

$$\begin{aligned}
\zeta_{CF} &= N_t^a[\zeta_d^0 + (\lambda_t^a)^2\zeta_p^0/2],\\
\zeta_{CF'} &= (N_t^a N_e^a)^{1/2}[\zeta_d^0 - \lambda_t^a\lambda_e^a\zeta_p^0/2],\\
k_{CF} &= N_t^a[1 + (\lambda_t^a)^2/2],\\
k_{CF'} &= (N_t^a N_e^a)^{1/2}[1 - \lambda_t^a\lambda_e^a/2 - A\lambda_t^a\lambda_s^a/2],\\
k_{CT'} &= (N_t^a N_e^b)^{1/2}[1 - \lambda_e^a + \lambda_t^a - 2\lambda_t^a S_t S_e + \lambda_t^a\lambda_e^a S_t/2\\
&\quad + A\lambda_t^b\lambda_s^a/2], \qquad (1)
\end{aligned}$$

Here ζ_d^0 and ζ_p^0 are, respectively, the spin-orbit coupling coefficients of the $3d^3$ ion and the ligand in free states. N_γ^x and λ_γ^x (or λ_s^x) are the normalization factors and the orbital admixture coefficients, with the superscripts x (= a and b) denoting the anti-bonding and bonding orbitals and the subscripts γ (= t and e) labeling the cubic (O_h) irreducible representations T_{2g} and E_g, respectively. The subscripts CF and CT represent the related quantities of the CF and CT mechanisms, respectively. A stands for the integral $R\langle\chi_s|\partial/\partial x|\chi_{px}\rangle$ between the ligand 3s and 3p orbitals, with the reference impurity-ligand distance R. The molecular orbital coefficients N_γ^x and λ_γ^x are usually determined from the normalization conditions, the orthogonality relationships, the approximate relationships for the anti-bonding orbitals and in terms of the effective covalency factor N based on the cluster approach [18,19].

2.2. Perturbation formulas for an orthorhombically distorted $3d^3$ cluster

For this strongly covalent system, not only the contributions from the conventional CF mechanism (related to the anti-bonding orbitals) but also those from the CT mechanism (related to the bonding and non-bonding orbitals) affect significantly the g-shifts arising from the second-order perturbation term due to the combination of spin-orbit coupling and orbital angular momentum interactions [18,19]. As for ZFSs D and E, the CF contributions originate from the third- and fourth- order perturbation terms due to the combination of orthorhombic CF and spin-orbit coupling interactions or the off-diagonal parts of the inter-electronic repulsion interactions, while the CT ones arise mainly from the third order perturbation terms due to the combination of orthorhombic CF and spin-orbit coupling interactions. Utilizing the Macfarlane's perturbation-loop method [20,21] and involving the CT contributions to g factors and the ZFSs D and E, one can obtain the improved perturbation formulas of the SHPs for an orthorhombically distorted octahedral $3d^3$ cluster as follows:

$$\begin{aligned}
D &= D_{CF} + D_{CT},\\
D_{CF} &= (35/9)\zeta_{CF}{}'^2 D_t(1/E_1^2 - 1/E_3^2) - 35BD_t\zeta_{CF}{}'\zeta_{CF}/(E_2E_3^2) + \zeta_{CF}{}'^2\{(49/216)[(175D_t^2 + 144D_\eta^2)/E_1^3\\
&\quad + 2(25D_t^2 + 144D_\eta^2)/E_3^3] + 4[(D_s + 5D_t/4)^2 + (D_\xi + D_\eta)^2][1/(E_1^2E_4) + 2/(E_3^2E_8)]\}\\
&\quad + \zeta_{CF}\zeta_{CF}{}'^2\{(35D_t/108)[2/E_1^3 + 2/E_3^3 - 4/(E_1^2E_3) + 5/(E_1E_3^2) + 5/(E_1E_3^2)] + (2/3)(D_s + 5D_t/4)\\
&\quad \times [2/(E_1^2E_4) + 1/(E_1E_3E_4)]\},\\
D_{CT} &= -(9/4)D_t\zeta_{CT}{}'^2/E_n^2;\\
E &= E_{CF} + E_{CT},\\
E_{CF} &= (-28\zeta_{CF}{}'^2/9)D_\eta(1/E_1^2 - 1/E_3^2) + 28BD_\eta\zeta_{CF}{}'\zeta_{CF}/(E_2E_3^2) - \zeta_{CF}{}'^2\{(490D_tD_\eta/27)(1/E_1^3 - 1/E_3^3)\\
&\quad - (16/3)(D_s + 5D_t/4)(D_\zeta + D_\eta)[1/(E_1^2E_4) - 1/(E_3^2E_8)]\} + \zeta_{CF}{}'^2\zeta_{CF}\{(7D_\eta/27)[2/E_3^3 - 1/E_1^3\\
&\quad - 12/(E_1^2E_3) + 5/(E_1E_3^2)] + (2/3)(D_\zeta + D_\eta)[1/(E_1^2E_4 + 1/(E_1E_3E_4)]\},\\
E_{CT} &= -(48/50)D_\eta\zeta_{CT}{}'^2/E_n^2;\\
g_x &= g_s + \Delta g_x^{CF} + \Delta g_x^{CT},
\end{aligned}$$

$$
\begin{aligned}
\Delta g_x^{CF} &= -8k_{CF}'\zeta_{CF}'/(3E_1) + [2(k_{CF}-2_{g_s})\zeta_{CF}{}^2 - 4k_{CF}'\zeta_{CF}'\zeta_{CF}]/9E_1^2 \\
&\quad + 4\zeta\zeta_{CF}{}'^2(k_{CF}-2g_s)/9E_3^2 - 2\zeta_{CF}{}'^2(k_{CF}+g_s)/3E_2^2 + 4k_{CF}'\zeta_{CF}'\zeta_{CF}[1/(9E_1E_3) - 1/(3E_1E_2) + 1/(3E_2E_3)] \\
&\quad + 16k_{CF}'D_\eta\zeta_{CF}'/9E_1^2 - 2k_{CF}'\zeta_{CF}'(35D_t + 7D_\xi + 7D_\eta)/9E_1^2, \\
\Delta g_x^{CT} &= 8\zeta_{CT}'k_{CT}'/(3E_n) - 9\zeta_{CT}'k_{CT}'[(5D_t - 3D_s) + 5(3D_\xi - 4D_\eta)/3]/E_n^2; \\
g_y &= g_s + \Delta g_y^{CF} + \Delta g_y^{CT}, \\
\Delta g_y^{CF} &= -8k_{CF}'\zeta_{CF}'/(3E_1) + [2(k_{CF}'-2g_s)\zeta_{CF}{}^2 - 4k_{CF}'\zeta_{CF}'\zeta_{CF}']/9E_1^2 + 4\zeta_{CF}{}'^2(k_{CF}-2g_s)/9E_3^2 \\
&\quad - 2\zeta_{CF}{}'^2(k_{CF}+g_s)/3E_2^2 + 4k_{CF}'\zeta_{CF}'\zeta_{CF}[1/(9E_1E_3) - 1/(3E_1E_3) + 1/(3E_2E_3)] \\
&\quad + 16k_{CF}'D_\eta\zeta_{CF}'/9E_1^2 - 2k_{CF}'\zeta_{CF}'(35D_t - 7D_\xi + 7D_\eta)/9E_1^2, \\
\Delta g_y^{CT} &= 8\zeta_{CT}'k_{CT}'/(3E_n) - 9\zeta_{CT}'k_{CT}'[(5D_t - 3D_s) - 5(3D_\xi - 4D_\eta)]/E_n^2; \\
g_z &= g_s + \Delta g_z^{CF} + \Delta g_z^{CT}, \\
\Delta g_z^{CF} &= -8k_{CF}'\zeta_{CF}'/(3E_1) + [2(k_{CF}-2g_s)\zeta_{CF}{}^2 - 4k_{CF}'\zeta_{CF}'\zeta_{CF}]/9E_1^2 \\
&\quad + 4\zeta_{CF}{}'^2(k_{CF}-2g_s)/9E_3^2 - 2\zeta_{CF}{}'^2(k_{CF}+g_s)/3E_2^2 + 4k_{CF}'\zeta_{CF}'\zeta_{CF}[1/(9E_1E_3) \\
&\quad - 1/(3E_1E_2) + 1/(3E_2E_3)] + 16k_{CF}'D_\eta\zeta_{CF}'/9E_1^2, \\
\Delta g_z^{CT} &= 8\zeta_{CT}'k_{CT}'/(3E_n) - 18\zeta_{CT}'k_{CT}'(5D_t - 3D_s)/E_n^2.
\end{aligned} \tag{2}
$$

The quantities D_s, D_t, D_ξ and D_η are the orthorhombic CF parameters. The corresponding denominators E_i ($i = 1 \sim 4$ and 8) [20,22] are the energy differences between the ground $^4A_{2g}$ and the excited $^4T_{2g}[t_2^2(^3T_1)e]$, $^2T_{2g}(t_2^3)$, $^2T_{2g}[t_2^2(^3T_1)e]$, $^4T_{1g}[t_2^2(^3T_1)e]$ and $^2T_{1g}[t_2^2(^3T_1)e]$ states, respectively. These denominators are expressed in terms of the cubic CF parameter Dq and Racah parameters B and C from the strong field approach [23,24]:

$$
\begin{aligned}
&E_1 \approx 10D_q, \quad E_2 \approx 15B + 4C, E_3 \approx 9B + 3C + 10Dq, \\
&E_4 \approx 10D_q + 12B, \quad E_8 \approx 10D_q + 6B.
\end{aligned} \tag{3}
$$

For an octahedral $3d^3$ cluster, the CT level can be determined as $E_n \approx 30000[\chi(L) - \chi(M)] + 14B$ (cm^{-1}) [15]. Here $\chi(L)$ and $\chi(M)$ are the optical electronegativities of ligand and central ions, respectively.

3. Calculations for the orthorhombic Cr^{3+} centre in K_2PdCl_4

The host K^+ site in K_2PdCl_4 is surrounded by a tetragonally compressed chlorine octahedron, with the cation-anion distances $R_x = R_y \approx 5.7689$ Å and $R_z \approx 3.2191$ Å [14]. Occupation of the impurity Cr^{3+} on host K^+ site can lead to the significant lattice modifications of the local impurity-ligand distances due to the remarkable discrepancies between charge and ionic radii of Cr^{3+} and K^+. For convenience, the local structure of the Cr^{3+} centre is described by a relative axial compression ratio ρ and a relative perpendicular bond length variation ratio τ (see Fig. 1). Usually, the effective (average) impurity-ligand bond length R in the impurity

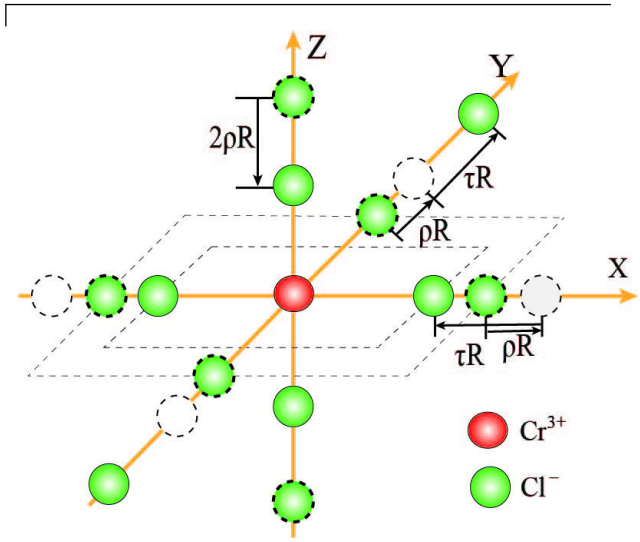

FIGURE 1. Local structure of the orthorhombic Cr^{3+} centre on K^+ site in K_2PdCl_4.

centre may differ from that of the host cation-anion distance $R_H(= (R_{\|H} + 2R_{\perp H})/3 \approx 4.919$ Å [14]) in K_2PdCl_4 since the ionic radius r_i (≈ 0.615 Å [25]) of the impurity Cr^{3+} is much smaller than the radius r_h (≈ 1.38 Å [25]) of the host K^+. The investigations based on experimental superhyperfine constant and extended X-ray absorption fine structure (EXAFS) measurements [26] reveal that the empirical relationship $R \approx R_H + (r_i - r_h)/2$ is approximately valid for an impurity ion in crystals. In view of the size mismatch, the reference bond length $R(\approx 4.537$ Å) is obtained for the stud-

ied system. Thus, the local impurity-ligand distances along X, Y and Z axes in the impurity centre can be expressed in terms of the reference bond length R and the local distortion parameters ρ and τ as follows:

$$R'_x = R(1+\rho-\tau), \quad R'_y = R(1+\rho+\tau),$$
$$R'_z = R(1-2\rho). \tag{4}$$

Utilizing the local geometry and the superposition model [27-31], the orthorhombic CF parameters can be determined as:

$$D_s = -2\bar{A}_2(R)/7[(R/R_x)^{t2} + (R/R_y)^{t2} - 2(R/R_z)^{t2}],$$
$$D_t = 8\bar{A}_4(R)/21[-(R/R_x)^{t4} - (R/R_y)^{t4} + 2(R/R_z)^{t4}],$$
$$D_\xi = 2\bar{A}_2(R)/7[(R/R_x)^{t2} - (R/R_y)^{t2}],$$
$$D_\eta = 5\bar{A}_4(R)/21[(R/R_x)^{t4} - (R/R_y)^{t4}]. \tag{5}$$

Here $t_2 \approx 3$ and $t_4 \approx 5$ [32] are the power-law exponents. $\bar{A}_2(R)$ and $\bar{A}_4(R)$ are the intrinsic parameters, with the reference distance R. The relationships $\bar{A}_4(R) \approx (3/4)Dq$ and $\bar{A}_2(R) \approx 10.8\bar{A}_4(R)$ [32-34] for $3d^n$ ions under octahedral CFs based on the superposition model are reasonably employed here.

In the light of the optical spectral measurements for Cr^{3+} in K_2PdCl_4 [14] and similar chlorides [35], the cubic field parameter $Dq \approx 1851$ cm^{-1} and the effective covalency factor $N \approx 0.82$ are obtained for the studied impurity centre. Utilizing the Slater-type self-consistent field wave functions [36] and the distance R, the group overlap integrals ($S_{dpt} \approx 0.00005$, $S_{dpe} \approx 0.0002$ and $S_{ds} \approx 0.00004$) and the integral $A \approx 2.1138$ are calculated. The related molecular orbital coefficients are determined for both CF and CT mechanisms from the cluster approach [18,19]: $N_t^a \approx 0.67$, $N_e^a \approx 0.670$, $\lambda_t^a \approx 0.702$, $\lambda_e^a \approx 0.688$, $\lambda_s^a \approx 0.138$ and $N_t^b \approx 0.663$, $N_e^b \approx 0.724$, $\lambda_t^b \approx -0.712$, $\lambda_e^b \approx -0.605$ and $\lambda_s^b \approx -0.121$. Appling the free-ion values ζ_d^0 (Cr^{3+})$\approx$ 273 cm^{-1} [37] and ζ_p^0 (Cl^-) $\approx$ 587 cm^{-1} [38], the spin-orbit coupling coefficients and the orbital reduction factors are obtained for both mechanisms from Eq. (1): $\zeta_{CF} \approx 280$ cm^{-1}, $\zeta_{CF'} \approx 88$ cm^{-1}, $\zeta_{CT'} \approx 396$ cm^{-1} and $k_{CF} \approx 0.835$, $k_{CF'} \approx 0.44$ and $k_{CT'} \approx 0.634$. The Racah parameters B and C in Eq. (3) can be expressed in terms of the free-ion values B_0 (≈ 1030 cm^{-1} [37]) and C_0 (≈ 3850 cm^{-1} [37]) of Cr^{3+} as: $B \approx B_0N^2$ and $C \approx C0N2$ [39]. The CT level E_n can be obtained from the values χ(Cl^-)$\approx$ 2.4 and χ(Cr^{3+}) $\approx$ 1.9 [15]. Substituting these values into Eq. (4) and fitting the calculated SHPs to the observed values, the optimal local distortion parameters ρ and τ are obtained:

$$\rho \approx 11.1\% \quad \text{and} \quad \tau \approx 11.1\% \tag{6}$$

The corresponding theoretical SHPs (Calc. ^{c}) are collected in Table I. The results (Calc. ^{a}) based on the host structural data of K^{3+} site in K2PdCl4 and inclusion of both the CF and CT contributions and those (Calc.^{b}) based on the above optimal local distortion parameters and inclusion of merely the CF contributions are also listed in Table I.

TABLE I. The ZFSs D and E (in 10^{-4} cm^{-1}) and g factors for Cr^{3+} in K_2PdCl_4.

	D	E	g_x	g_y	g_z
Calc.^{a}	28178	0	2.178	2.178	2.338
Calc.^{b}	22849	746	1.994	1.994	1.997
Calc.^{c}	89	21	2.078	2.165	2.220
Expt. [14]	89(2)	19(2)	2.096(2)	2.167(2)	2.220(2)

^{a}Calculations based on the host structural data of K^+ site in K_2PdCl_4 and inclusion of both the CF and CT contributions.

^{b}Calculations based on the optimal local distortion parameters ρ and τ and inclusion of merely the CF contributions.

^{c}Calculations based on the optimal local distortion parameters ρ and τ and inclusion of both the CF and CT contributions.

4. Discussion

Table I indicates that the theoretical SHPs (Calc. c) based on the local distortion parameters ρ and τ show better agreement with the experimental data than those (Calc. a) based on the host structural data of K^+ site and those (Calc. ^{b}) based on omission of the CT contributions. Thus, the measured EPR spectra for the Cr^{3+} centre in K_2PdCl_4 are satisfactorily explained in a uniform way. Meanwhile, the information about the local distortion around the impurity Cr^{3+} is theoretically determined by analyzing the experimental ZFSs. The following points are discussed here.

(1) As compared with the axial compression ratio ($\rho_H \approx 18.6\%$) and nearly zero perpendicular distortion ratio ($\tau_H \approx 0$) of the host K^+ site in K_2PdCl_4, the impurity Cr^{3+} centre exhibits smaller axial compression ($\rho \approx 11.1$ %) and much larger perpendicular distortion ($\tau \approx 11.7$ %) and hence a more regular ligand octahedron, corresponding to the very small D and E. Thus, the much (two or three order in magnitude) larger D and zero E (Calc. ^{a}) based on the structural data of host K^+ site can be understood. The microscopic mechanisms of the local lattice deformations are illustrated as the much stronger Cr^{3+}-Cl^- interaction than the host K^+-Cl^- combination due to the much higher impurity valence state. Meanwhile, the long reference impurity-ligand distance $R(\approx 4.537$ Å) and hence low force constant of the Cr^{3+}-Cl^- bonds also account for the above remarkable Cr^{3+}-Cl^- bond length variations with respect to the host K^+-Cl^- bonds. As a result, the axial and perpendicular distortions are considerably decreased and increased, respectively, from host K^+ site to the impurity centre. As one might deliberately assign the measured EPR signals to Cr^{3+} on the square planar Pd^{2+} site, the calculated D would be much (two or three order in magnitude) larger than the

experimental value, and the above remarkable discrepancy cannot be removed by adjusting the related spectral parameters or local distortion parameters. So, Cr^{3+} may tend to occupy the octahedral K^+ site instead of the square planar Pd^{2+} site and is quite different from the conventional tetragonal Cu^{2+} centre on Pd^{2+} site in K_2PdCl_4 [40]. This point can be illustrated by the dissimilar electron configurations of Cu^{2+} ($3d^9$) and Cr^{3+} ($3d^3$), which tend to exhibit square planar $[CuX_4]$ and octahedral $[CrX_6]$ groups by means of dsp^2 and d^2sp^3 hybrid orbitals [41,42]. Interestingly, similar octahedral trivalent Fe^{3+} ($3d^5$) centre on K^+ site was also reported for iron doped K_2PdCl_4 [43], which can also be ascribed to the octahedral $[FeCl_6]$ group by means of sp^3d^2 hybrid orbitals [41,42]. It seems that electronic configuration plays a more important role than size or charge mismatch in occupation of transition-metal impurities in K_2PdCl_4. So, the impurity Cr^{3+} occupying K^+ site rather than Pd^{2+} site is understandable in physics.

(2) When the CT contributions are ignored, the calculated g factors and ZFSs (Calc. ^{b}) are smaller and much larger than the experimental data. For the studied $[CrCl_6]$ group, the system demonstrates strong covalency due to the covalent ligand Cl^- and central ion Cr^{3+} with high valence state and much larger $\zeta_p^0(Cl^-) \approx 587$ cm^{-1} [38] than ζ_d^0 (Cr^{3+}) ≈ 273 cm^{-1} [37]. Substantially, the host K_2PdCl_4 may exhibit strong covalency due to the optical electronegativity (≈ 2.2 [15]) of Pd^{2+} comparable with that (≈ 3.0 [15]) for Cl^-. This can be illustrated by the effective covalency factor N (≈ 0.82) and the obvious orbital admixture coefficients ($\approx 0.2 \sim 0.7$) from the cluster approach. In fact, the contributions to g-shifts Δ_{gCT} from the CT mechanism are opposite in sign and twenty-one times larger in magnitude compared with Δ_{gCF} from the CF mechanism. As for the ZFSs, the CT contributions D_{CT} and E_{CT} are opposite in sign and almost the same (characterized by the ratios $|D_{CT}/D_{CF}| \approx 99.6\%$ and $|E_{CT}/E_{CF}| \approx 99.3\%$) in magnitude with respect to the corresponding D_{CF} and E_{CF}. Thus, the CT contributions are found to be important and should be included in the EPR analysis.

(3) The errors of the present theoretical calculations may be analyzed as follows. First, the final results may be brought forward some errors due to the approximations of the theoretical model and formulas based on the spin Hamiltonian theory, in which only the contributions from the nearest neighbor ligands are considered whereas the influences of the ions in the outer ligand spheres are omitted. For the present impurity Cr^{3+} in tetragonal K_2PdCl_4 lattice, the electric fields from the rest ions of the crystal could be anisotropic and bring forward some influences on the total crystal fields acting upon Cr^{3+}. To some extent, the opposite contributions to the crystal fields arising from the relevant ions (*e.g.*, Pd^{2+}, Cl^-; K^+, Cl^-; etc.) may partially cancel each other due to opposite charges and lead to insignificant effects on the total crystal fields of Cr^{3+} because of their successively farther distances ($\gg R \approx 4.537$ Å) from the impurity. Second, the error of the reference impurity-ligand distance R may arise from the empirical relationship in terms of the difference between the ionic radii of the impurity and the replaced cation [26]. Fortunately, the influences of R is actually cancelled in the calculations of the orthorhombic CF parameters in Eq. (5), and the above error of R would merely affect the related group overlap integrals and lead to even smaller errors (no more than 0.5%) for the resultant SHPs and the optimal local distortion parameters ρ and τ. Third, substitution of K^+ by Cr^{3+} with two extra positive charge may induce some means of charge compensators (*e.g.*, one Pd^{2+} vacancy or two K^+ vacancies) and might slightly modify the local structure of the impurity centre. However, the non-axial charge compensators would lead to considerable perpendicular orthorhombic distortion and significant E, which was obviously inconsistent with the experimental tiny E value [14]. On the other hand, the possible axial compensators (*e.g.*, Pd^{2+} and K^+ vacancies) might bring forward important effect on the charge distribution of the impurity centre. However, the negative effective charges of these possible compensators would repel the axial ligand(s) Cl^- towards the central Cr^{3+}, inducing much more axial compression of the impurity centre and hence larger magnitude of D. Nevertheless, this is actually in disagreement with the observed very small D [14]. So, the possible charge compensators may occur far from the impurity and its influence on the local structure is very small and negligible. Finally, the empirical superposition model and ratio $\bar{A}_2(R)/\bar{A}_4(R) \approx 10.8$ for the intrinsic parameters of other systems would also result in some errors. Based on the calculations, when the ratio varies within the widely accepted range of $9 \sim 12$, the errors for the SHPs and the optimal distortion parameters are estimated to be less than 4%. In fact, the above treatments need to be justified for the certain case, especially those with nearby charge compensation. Therefore, in order to perform more accurate studies of the SHPs for the present system, more powerful density function theory (DFT) calculations are to be adopted in the future work.

5. Conclusions

The SHPs and local structure for Cr^{3+} in K_2PdCl_4 are theoretically analyzed from the perturbation calculations for an orthorhombically distorted $3d^3$ cluster. The impurity Cr^{3+} is found not to occupy the host Pd^{2+} site but to locate at the octahedral K^+ site, associated with the relative axial compres-

sion ratio ρ ($\approx$ 11.1%) and the relative perpendicular bond length variation ratio τ ($\approx$ 11.7%). So, the impurity centre exhibits smaller axial compression distortion and much larger perpendicular orthorhombic distortion than the host K^+ site in K_2PdCl_4 and hence a more regular ligand octahedron, corresponding to the very small D and E. The contributions to g-shifts Δg_{CT} from the CT mechanism are opposite in sign and twenty-one times larger in magnitude compared with Δg_{CF} from the CF mechanism. For the ZFSs, the CT contributions DCT and ECT are opposite in sign and almost the same in magnitude with respect to the corresponding DCF and ECF. The microscopic mechanism for this unique Cr^{3+} centre on octahedral K^+ site, which is quite dissimilar to the conventional tetragonal Cu^{2+} centre on square planar Pd^{2+} site, is illustrated in view of the d^2sp^3 hybrid orbitals.

Acknowledgments

This work was financially supported by the Key Project of Sichuan Education Department [17ZA0050], the Science Project of Chengdu Normal University [RCYJ2016-2], the Sichuan Province Academic and Technical Leaders Support Fund [Y02028023601041] and the National Natural Science Foundation of China under granted no. 11764028.

1. A. Garoufis, S.K. Hadjikakou, and N. Hadjiliadis, *Coordin. Chem. Rev.* **253** (2009) 1384-1397.
2. B. Karmakar and J. Benerji, *Tetrahedron Lett.* **51** (2010) 2748-2750.
3. C. Vannini *et al.*, *Aquat Toxicol.* **102** (2011) 104-113.
4. Z. Pan, Y.Y. Lu and F. Liu, *Nat. Mater.* **11** (2012) 58-63.
5. H. Aizawa *et al.*, *Meas. Sci. Technol.* **15** (2004) 1484-1489.
6. D. Bravo and F.J. López, *Opt. Mater.* **13** (1999) 141-145.
7. A. Ikesue, K. Kamata, and K. Yoshida, *J. Am. Chem. Soc.* **78** (1995) 2545-2547.
8. J. Zhu *et al.*, *Appl. Catal. B* **62** (2006) 329-335.
9. X.S. Wang *et al.*, *RSC Adv.* **5** (2015) 12886-12889.
10. D. Mohan, C.U. Pittman, and J. Hazard, *Mater.* **137** (2006) 762-811.
11. C. Cervantes *et al.*, *FEMS Microbiol. Rev.* **25** (2001) 335-347.
12. D.A. Eastmond, J.T. MacGregor, and R.S. Slesinski, *Crit. Rev. Toxicol.* **38** (2008) 173-190.
13. S.H. Liu, F. Lu, and J.J. Zhu, *Chem. Commun.* **47** (2011) 2661-2663.
14. R. Kripal and S.D. Pandey, *Appl. Magn. Reson.* **45** (2014) 731-742.
15. A.B.P. Lever, *Inorganic Electronic Spectroscopy* (Elsevier Science Publishers, Amsterdam, 1984).
16. J.A. Aramburu and M. Moreno, *J. Chem. Phys.* **79** (1983) 4996-4999.
17. J.A. Aramburu and M. Moreno, *Solid State Commun.* **62** (1987) 513-516.
18. M.Q. Kuang, S.Y. Wu, B.T. Song, L.L. Li, and Z.H. Zhang, *Optik* **124** (2013) 892-896.
19. Y.X. Hu, S.Y. Wu, and X.F. Wang, *Philosoph. Mag.* **90** (2010) 1391-1400.
20. R.M. Macfarlane, *Phys. Rev. B.* **1** (1970) 989-1004.
21. S.Y. Wu and W.C. Zheng, *J. Phys. Condens. Matter.* **10** (1998) 7545-7551.
22. R.M. Macfarlane, *J. Chem. Phys.* **47** (1967) 2066-2073.
23. S.Y. Wu, L.H. Wei, Z.H. Zhang, and X.F. Wang, *Spectrochim. Acta A* **71** (2009) 2023-2025.
24. H.M. Zhang, S.Y. Wu, P. Xu, and L.L. Li, *J. Mol. Struc.: Theo. Chem.* **953** (2010) 157-162.
25. R.D. Shannon, *Acta Crystallogr. A* **32** (1976) 751-767.
26. M. Moreno, M.T. Barriuso, and J.A. Aramburu, *Appl. Magn. Reson.* **3** (1992) 283-304.
27. D.J. Newman, and B. Ng, *Rep. Prog. Phys.* **52** (1989) 699-763.
28. H.N. Dong, and X.S. Liu, *Mol. Phys.* **113** (2015) 492-496.
29. H.M. Zhang, S.Y. Wu, M.Q. Kuang, and Z.H. Zhang, *J. Phys. Chem. Solids* **73** (2012) 846-850.
30. X.F. Hu, S.Y. Wu, G.L. Li, and Z.H. Zhang, *Mol. Phys.* **112** (2014) 2627-2632.
31. H.M. Zhang, S.Y. Wu, and P. Xu, *Can. J. Phys.* **89** (2011) 177-183.
32. D.J. Newman, D.C. Pryce, and W.A. Runciman, *Am. Mineral.* **63** (1978) 1278-1281.
33. C. Rudowicz, Z.Y. Yang, Y.Y. Yeung, and J. Qin, *J. Phys. Chem. Solids.* **64** (2003) 1419-1428.
34. S.Y. Wu, H.M. Zhang, P. Xu, and S.X. Zhang, *Spectrochim. Acta A* **75** (2010) 230-234.
35. W. Ulrici, *Phys. Stat. Solidi* **27** (1968) 489-500.
36. E. Clementi, D.L. Raimondi, and W.P. Reinhardt, *J. Chem. Phys.* **47** (1967) 1300-1307.
37. J.S. Griffith, *The Theory of Transition-Metal Ions*, Cambridge University Press, London, 1964.
38. D.W. Smith, *J. Chem. Soc. A* (1970) 3108-3120.
39. M.G. Zhao, J.A. Xu, G.R. Bai, and H.S. Xie, *Phys. Rev. B.* **27** (1983) 1516-1522.
40. C. Chow, K. Chang, and R.D. Willett, *J. Chem. Phys.* **59** (1973) 2629-2640.
41. C.K. Jørgensen, *Absorption Spectra and Chemical Bonding in Complexes*, Pergamon Press, New York, 1962.
42. A.S. Chakravarty, *Introduction to the Magnetic Properties of Solids*, (Wiley-Interscience Publication, New York, 1980).
43. R. Kripal and S.D. Pandey, *Chinese J. Phys.* **52** (2014) 1686-1701.